Journal of Hazardous Materials 178 (2010) 517–521

Contents lists available at ScienceDirect

Journal of Hazardous Materials

journal homepage: www.elsevier.com/locate/jhazmat

Preparation, characterization, photocatalytic properties of titania hollow sphere doped with cerium

Chao Wang[a,b], Yanhui Ao[a,b,*], Peifang Wang[a,b], Jun Hou[a,b], Jin Qian[a,b], Songhe Zhang[a,b]

[a] Key Laboratory of Integrated Regulation and Resource Development on Shallow Lakes, Ministry of Education, College of Environmental Science and Engineering, Hohai University, Nanjing, 210098, China
[b] State Key Laboratory of Hydrology-Water Resources and Hydraulic Engineering, Hohai University, Nanjing, 210098, China

ARTICLE INFO

Article history:
Received 12 October 2009
Received in revised form 20 January 2010
Accepted 21 January 2010
Available online 25 January 2010

Keywords:
Ce-doped
Hollow sphere
Titania
Photocatalysis

ABSTRACT

Ce-doped titania hollow spheres were prepared using carbon spheres as template and Ce-doped titania nanoparticles as building blocks. The Ce-doped titania nanoparticles were synthesized at low temperature. The prepared hollow spheres were characterized by X-ray diffraction (XRD), transmission electron microscope (TEM), X-ray photoelectron spectroscopy (XPS) and UV–vis diffuse reflectance spectrum (DRS). The effect of Ce content on the physical structure and photocatalytic properties of doped titania hollow sphere samples was investigated. Results showed that there was an optimal Ce-doped content (4%) for the photocatalytic activity of X-3B degradation. The apparent rate constant of the best one was almost 31 times as that of P25 titania. The mechanism of photocatalytic degradation of dyes under visible light irradiation was also discussed.

1. Introduction

Semiconductor photocatalysts have been attracting considerable attention for a long time in the fields of catalysis, electrochemistry and photochemistry. That can be attributed to their significant effects on solving environmental problems (such as air or water pollution) [1–4]. Among various semiconductor photocatalyst, titania has been proved to be the most suitable catalysts for widespread environmental application because of its biological and chemical inertness, strong oxidizing power, non-toxicity and long-term stability against photo and chemical corrosion [5–10]. However, its technological application seems to be limited by several factors. The most restrictive one is the need of using ultraviolet (UV, wavelength (λ) < 387 nm) as excitation source due to the wide band gap of titania (3.2 eV for anatase) [11]. Therefore, only less than 5% of the solar irradiance at the Earth's surface can be captured by titania.

For the sake of efficient utilization of sunlight, the technology of enlarging the absorption scope of TiO_2 appears as an appealing challenge. Therefore, the developing of new generation photocatalysts is important. There are many methods for the preparation of visible light responsive photocatalyst such as doping of titania with nonmetal [12–15]. More recently, doping of titania with lanthanide ions has also attracted much attention. This method not only extends the photo-response to visible regions, but also improves the separation efficiency of photo-induced electron–hole pairs of titania [16–20]. On the other hand, it is well known that morphology and microstructures are very important to the photocatalytic activity of titania. Therefore, there are many papers focused on the new structures of titania such as nanorods [21,22], nanowires [23,24], nanotubes [25,26] and so on. Recently, fabrication of titania hollow microspheres has also attracted enormous attention because of their low density, large surface area, good surface permeability as well as high light-harvesting efficiencies [27].

In the present work, for the achievement of visible light responsive titania with high photocatalytic activity, we find a way for the preparation of Ce-doped titania hollow spheres. Then, we studied their photocatalytic activity on the decomposition of Reactive Brilliant Red dye X-3B (C.I. reactive red 2) in aqueous solution.

2. Experiment

2.1. Preparation of carbon spheres

In a typical synthesis of colloidal carbon spheres, 6 g of glucose was dissolved in 40 mL water to form a clear solution. The solution was then sealed in a 50 mL Teflon-lined autoclave and maintained at 180 °C for 4 h. The samples were then centrifuged, washed, and redispersed in water and ethanol for five cycles, respectively. The

* Corresponding author at: Key Laboratory of Integrated Regulation and Resource Development on Shallow Lakes, Ministry of Education, Hohai University, Nanjing 210098, China. Tel.: +86 25 83787330; fax: +86 25 83787330.
E-mail address: andyao@hhu.edu.cn (Y. Ao).

0304-3894/$ – see front matter © 2010 Elsevier B.V. All rights reserved.
doi:10.1016/j.jhazmat.2010.01.111

obtained carbon spheres were then dried at 80 °C for 2 h under vacuum.

2.2. Preparation of Ce-doped titania

Ce-doped titania was prepared as follows: 25 mL Ti $(OBu)_4$ diluted with 8 mL (i-PrOH) was dropwise added into aqueous solution dissolved with definite cerium nitrate, whose acidity was adjusted with HNO_3 (pH = 2). Then, the solution was kept under reflux condition (around 75 °C) for 24 h. Finally, Ce-doped TiO_2 sol was obtained after PrOH and n-butyl alcohol were removed from the solution in a rotatory evaporator under vacuum. In our experiment, four samples with cerium atom percent of 1%, 2%, 4% and 6% were prepared.

2.3. Preparation of Ce-doped titania hollow spheres (Ce-TH)

0.1 g carbon spheres were added into 30 mL Ce-doped titania sol prepared by above mentioned method. The suspension was stirred for 6 h under vacuum condition. Then the solids were centrifuged, washed by water for 3 times. Thus, Ce-doped titania coated carbon spheres were obtained. In order to produce Ce-doped titania hollow spheres of anatase, the titania–carbon composite particles were calcined at 500 °C for 3 h in the air. Then the obtained samples were defined as Ce-TH-1–Ce-TH-4 for Ce-doped titania hollow spheres with cerium ion percent of 1%, 2%, 4% and 6%, respectively.

2.4. Photocatalytic activity

In order to investigate the photocatalytic activity of as-prepared Ce-doped titania hollow spheres, degradation experiments of Reactive Brilliant Red X-3B (C.I. reactive red 2) were studied under visible light. 0.1 g of samples was dispersed into a 200 mL X-3B aqueous solution, which initial dye concentration is 25 mg L^{-1} and then irradiated with a 250 W halogen lamp (Instrumental Corporation of Beijing Normal University, with a light filter cutting off the light below 400 nm) under continuous stirring. Before the irradiation, the suspension was maintained in the dark for 1 h to reach complete adsorption–desorption equilibrium. The blank experiment without catalysts was also investigated, and the value can be neglected with less than 2% of conversion after 2 h illumination. The concentration of X-3B was determined by HPLC. The HPLC system was Agilent 1100 with tunable absorbance detector adjusted at 230 nm for the detection. A reverse-phase column (length, 250 mm; internal diameter, 4.6 mm) Aglient Eclipse XDB-C18 was used. The mobile phase was composed of methanol and ultra-pure water. The v/v ratio CH_3OH/H_2O was 70/30 and the flow rate was 0.6 mL min^{-1}.

2.5. Characterization

The structure properties were determined by X-ray diffractometer (XD-3A, Shimadazu Corporation, Japan) using graphite monochromatic copper radiation (Cu-Kα) at 40 kV, 30 mA over the 2θ range 20–80°. The morphologies were characterized by transmission electron microscopy (TEM, JEM2000EX). The UV–vis absorption spectra of the hollow titania spheres were observed with Shimadzu UV-2100 equipped with an integrating sphere. The binding energy was identified by X-ray photoelectron spectroscopy (XPS) with Mg-Kα radiation (ESCALB MK-II).

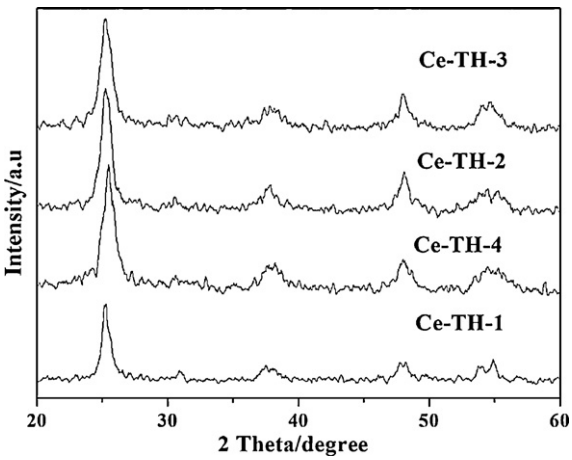

Fig. 1. XRD patterns of Ce-TH-1, Ce-TH-2, Ce-TH-3 and Ce-TH-4.

3. Results and discussion

3.1. Characterization of the prepared samples

The phase structures of the as-prepared samples were investigated by XRD method and the results are shown in Fig. 1. It can be seen that all samples exhibit only the characteristic peaks of anatase phase (major peaks: 25.4°, 38.0°, 48.0°, 54.7°). No crystalline phase ascribed to cerium oxides can be found in respect that the Ce content of our samples is below the detection limits of the XRD instrument, or the cerium species are dispersed well on the surface of titania nanoparticles. The average crystallite sizes of as-prepared samples can be calculated by applying the Debye-Scherrer formula on the anatase (1 0 1) diffraction peaks: [28]

$$D = \frac{K\lambda}{\beta \cos\theta} \quad (1)$$

where D is the crystalline size, λ the wavelength of X-ray radiation (0.1541 nm), K the constant usually taken as 0.89, and β is the peak width (in radians) at half-maximum height (PWHMH) after subtraction of equipment broadening, $2\theta = 25.4°$ for anatase phase titania. From the equation, we can see that the only parameter determines the crystal size is the peak width. Furthermore, from the figure we can see that the peak of 25.4° become wider and the intensity of this characterized peak become lower as the doping amount of cerium ion increases. Therefore, we can predict that the crystal size of the Ce-TH samples would become smaller as the doping amount of cerium ion increases. From Fig. 1, the data of PWHMH and the calculated average particle size are listed in Table 1. From the results, the size of the titania crystallites become smaller with the doping amount of cerium ion increases. It illustrates that cerium doping suppresses the crystallite growth of anatase titania. This is because the adsorption of cerium species on the surface of titania inhibits crystallites growth of titania nanoparticles.

Table 1
Different parameters of Ce-TH-1–Ce-TH-4.

Samples	PWHMH	Crystallite size (nm)	95% confidence interval	Apparent rate constant (min^{-1})	Real Ce content
Ce-TH-1	0.0129	10.9	(0.01039, 0.01131)	0.011	0.6%
Ce-TH-2	0.0138	10.2	(0.01100, 0.01227)	0.012	1.1%
Ce-TH-3	0.0154	9.2	(0.02536, 0.3254)	0.029	2.8%
Ce-TH-4	0.0169	8.3	(0.01025, 0.01193)	0.011	4.1%

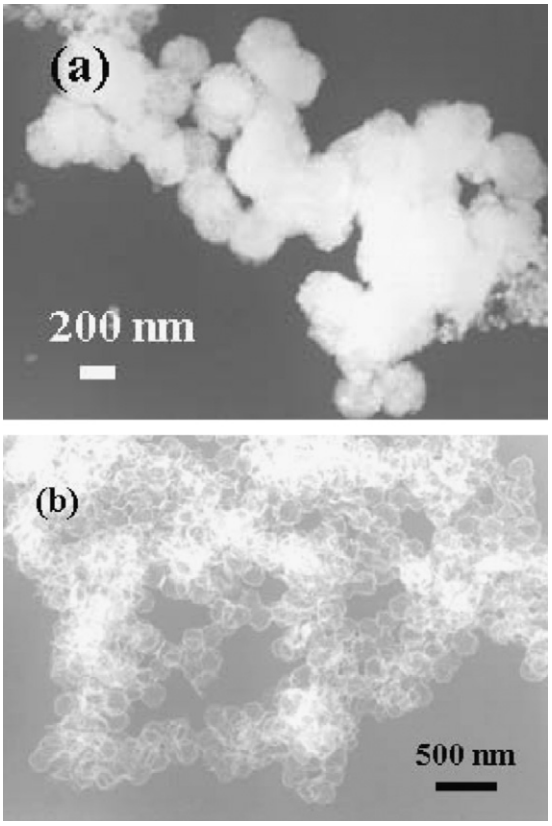

Fig. 2. TEM images of (a) Ce-doped titania coated carbon spheres and (b) Ce-TH-3.

The TEM images of different samples are shown in Fig. 2. Fig. 2(a) shows the morphology of titania coated carbon sphere nanocomposite (the precursor for Ce-TH-3). It can be seen that the titania nanoparticles dispersed uniformly on the surface of carbon spheres. Then, Fig. 2(b) shows the typical image of Ce-TH-3, it can be seen that there is a strong contrast between the edges and centers, which indicates that the hollow structure of titania spheres has been formed. The results illustrate that Ce-doped titania hollow spheres can be easily obtained by our method. Furthermore, the real contents of cerium in different samples were investigated by EDS. The obtained data are shown in Table 1, from which we can see that the real contents of cerium follow the same trend as the precursors. All samples show lower cerium content than corresponding precursors.

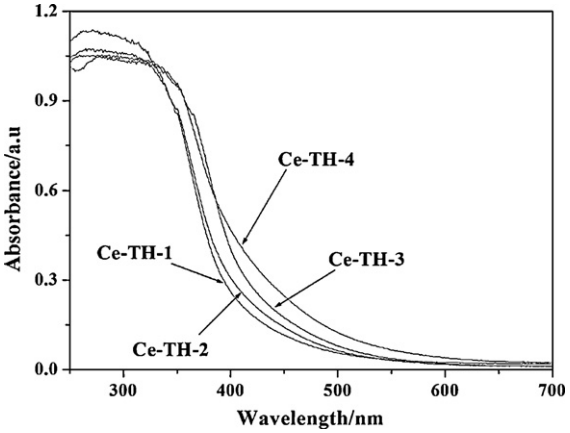

Fig. 3. The diffuse reflectance UV–vis spectra of Ce-TH-1, Ce-TH-2, Ce-TH-3 and Ce-TH-4.

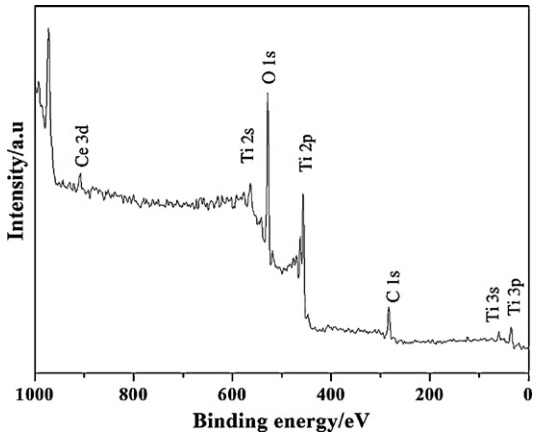

Fig. 4. XPS survey spectrum of Ce-TH-3.

Fig. 3 shows the UV–visible diffuse reflectance spectra of different Ce-doped titania hollow sphere samples. The results indicated that cerium doping by this method can give rise to a clear red-shift in the absorption band edge of the titania hollow spheres. High visible absorbance (400–500 nm) was observed for all Ce-doped samples. In addition, we can observe that the red-shift and visible absorbance of different samples enhanced as the doping amount of cerium increases (Nd-TH-4 > Nd-TH-3 > Nd-TH-2 > Nd-TH-1). The red-shift may be ascribed to the following reason: the energy level for Ce^{4+}/Ce^{3+} is 1.8 eV. Therefore, the doping of Ce causes the introduction of such energy level into the band gap of titania. This new energy level induces the red-shift through a charge transfer between impurity band and conduction band of titania [29,30].

The valence state of cerium ion in the titania hollow spheres was determined by X-ray photoelectron spectroscopy, which has been employed as an important characteristic method to detect the chemical states of different atom in doped titania samples [31,32]. The XPS survey spectrum of Ce-TH-3 (see Fig. 4) indicates that the peak contains Ti, O, C and Ce atoms. The carbon peak is attributed to the residual carbon from the sample and adventitious hydrocarbon from XPS instrument itself. Fig. 5 shows the high-resolution XPS spectra of Ce 3d. It can be seen that there are two major peaks centered at 885.7 and 904.9 eV, which represents Ce 3d 5/2 and 3d 3/2 orbits, respectively. The results demonstrated that Ce atoms exist in the form of +4 valences [33,34].

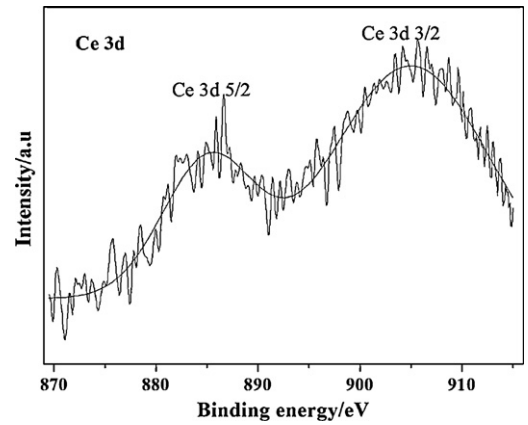

Fig. 5. High-resolution XPS spectrum of Ce 3d region of Ce-TH-3.

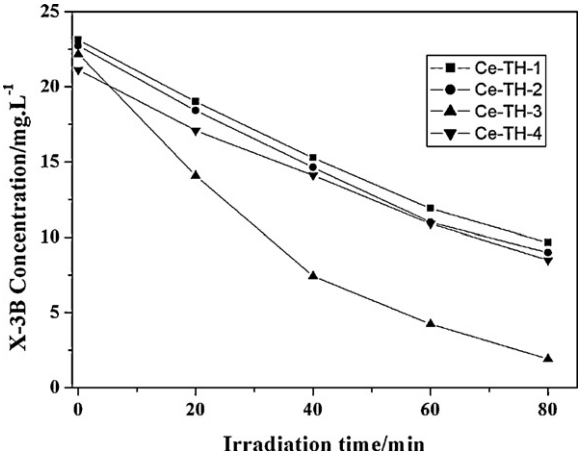

Fig. 6. Variation of X-3B concentration against time under visible light irradiation in the presence of Ce-TH-1, Ce-TH-2, Ce-TH-3 and Ce-TH-4.

3.2. Photocatalytic activity

Fig. 6 shows the variations of X-3B concentration against the irradiation time in the presence of different samples under visible light irradiation. From the figure, the concentration of X-3B decreased gradually as the exposure time increases. After 80 min irradiation, the degradation percent of X-3B are 61.3%, 64.0%, 92.3% and 66.0% for Ce-TH-1, Ce-TH-2, Ce-TH-3 and Ce-TH-4, respectively.

In addition, we investigated the kinetic process of X-3B degradation. It illustrates that photocatalytic degradation of X-3B as a function of the irradiation time in the presence of different samples follow first-order kinetic reaction as following:

$$r = \frac{dC}{dt} = k_{app}C \quad (2)$$

where r is the degradation rate of X-3B, C is the concentration of X-3B, k_{app} is the apparent reaction rate constant, t is the reaction time. From the above equation we can obtained the following equation:

$$\ln \frac{C_0}{C} = k_{app}t \quad (3)$$

C_0 is the initial concentration of X-3B before visible light irradiation. By Eq. (3), we are able to find the apparent reaction rate constant from the gradient of the graph of $\ln(C_0/C)$ against irradiation time. The apparent rate constant can be chosen as the basic kinetic parameter for the different photocatalysts since it enables one to determine a photocatalytic activity independent of the previous adsorption period in the dark and the concentration of X-3B remaining in the solution [35]. The corresponding linear transforms in $\ln(C_0/C)$ as a function of irradiation time are given in Fig. 7. From the figure, we can obtain the apparent rate constant of different samples. The obtained values are shown in Table 1. The apparent rate constants of Ce-TH samples are all much larger than that of P25 (0.00099 min^{-1}).

Under visible light irradiation, it is well known that there are two possible pathways contributing to the photo-degradation of X-3B molecules. The first pathway is related to the light absorption of Ce-doped titania under visible light regions. As mentioned in DRS section, the electrons can be excited from the valence band of Ce-doped titania samples into Ce 4*f* level under visible light irradiation. Then, the excited electrons of the semiconductor can react with the adsorbed oxygen to form oxidizing species which can bring about the photo-degradation of X-3B. The second possible pathway is photosensitization, in which it is the dye molecule but not titania was excited by visible light and generated an electron. Then, the excited electrons were transferred to the conduction band of titania

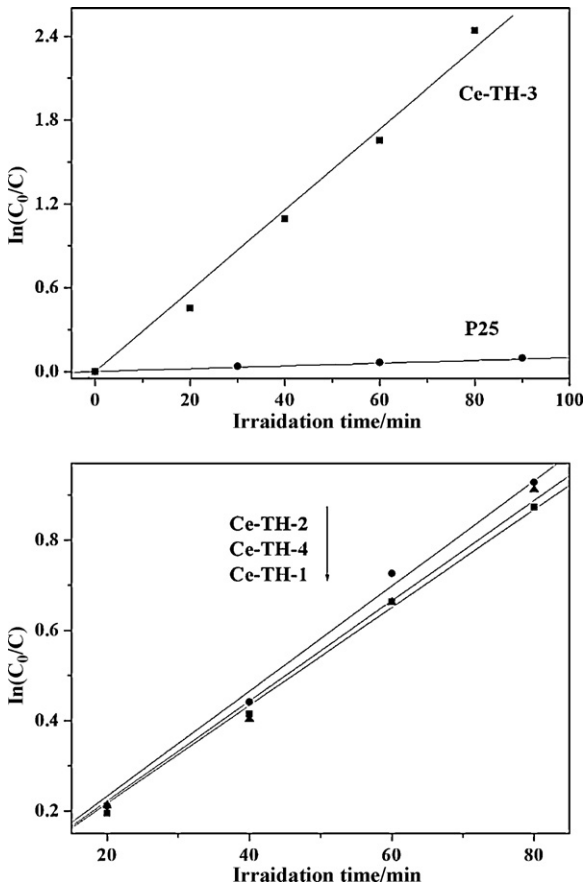

Fig. 7. Linear transform $\ln(C_0/C) = f(t)$ of the kinetic curves of X-3B disappearance for P25, Ce-TH-1, Ce-TH-2, Ce-TH-3 and Ce-TH-4 from Fig. 6.

due to the energy level of the excited state of the dyes is higher than that of titania conduction band. Afterwards, the electrons were transferred to adsorbed oxygen to form oxidizing species, which can degrade the X-3B molecule. By doping of titania by cerium, the excited electron can be trapped by Ce^{4+} ion through the following process:

$$Ce^{4+} + e^- \rightarrow Ce^{3+}$$

$$Ce^{3+} + O_2 \rightarrow Ce^{4+} + {}^{\bullet}O_2^-$$

Then, the electrons trapped in Ce^{4+}/Ce^{3+} site are transferred to the surrounding adsorbed oxygen. Therefore, the recombination rate of photo-induced electron–hole pairs is decreased and the photocatalytic activity of Ce-doped titania increased. However, there is an optimal Ce-doped content exists according to Xu et al. [29] and Li et al. [33]. That can be attributed to the following reason, when Ce-doped content increases further; it becomes the recombination center of photo-induced electron–hole pairs because the thickness of the space charge layer decreases with an increasing in dopant content. When this layer approximates the penetration depth of the light into the solid, all generated electron–hole pairs are efficiently separated [29]. According to the data of photocatalytic experiment, we can know that the optimal Ce-doped content is 4% (atom percent) for Ce-TH-3.

4. Conclusions

In summary, we report a simple method for the preparation of Ce-doped titania hollow spheres using carbon spheres as template. Results show that the Ce doping causes a red-shift of

absorption spectrum for titania. The photocatalytic activity of as-prepared hollow titania spheres with different Ce-doped content was determined by degradation of Reactive Brilliant Red dye X-3B (C.I. reactive red 2) under visible light irradiation. Results show that the obtained Ce-doped titania hollow sphere samples are all with high photocatalytic activity under visible light. In our work, it is found that the optimal Ce-doped content is 4% (atom percent).

Acknowledgments

We are grateful for grants from the national key basic research development program ("973" project) of China (no. 2009CB429006), University Natural Science Foundation of Jiangsu Education Bureau (Peifang Wang), Basic research project of Jiangsu province (BK2008041), China Postdoctoral Science Foundation (no. 20090450133).

References

[1] M.R. Hoffmann, S.T. Martin, W.Y. Choi, D.W. Bahnemann, Environmental applications of semiconductor photocatalysis, Chem. Rev. 95 (1995) 69–96.
[2] A. Fujishima, T.N. Rao, D.A. Tryk, Titanium dioxide photocatalysis, J. Photochem. Photobiol. C 1 (2000) 1–21.
[3] Y.X. Wang, X.Y. Li, N. Wang, X. Quan, Y.Y. Chen, Controllable synthesis of ZnO nanoflowers and their morphology-dependent photocatalytic activities, Sep. Purif. Technol. 62 (2008) 727–732.
[4] H.Y. Zhu, R. Jiang, L. Xiao, Y.H. Chang, Y.J. Guan, X.D. Li, G.M. Zeng, Photocatalytic decolorization and degradation of Congo Red on innovative crosslinked chitosan/nano-CdS composite catalyst under visible light irradiation, J. Hazard. Mater. 169 (2009) 933–940.
[5] A.L. Linsebigler, G.Q. Lu, J.T. Yates, Photocatalysis on TiO_2 surfaces: principles, mechanisms, and selected results, Chem. Rev. 95 (1995) 735–758.
[6] J.G. Yu, H.G. Yu, B. Cheng, X.J. Zhao, J.C. Yu, W.K. Ho, The effect of calcination temperature on the surface microstructure and photocatalytic activity of TiO_2 thin films prepared by liquid phase deposition, J. Phys. Chem. B 107 (2003) 13871–13879.
[7] J.C. Zhao, T.X. Wu, K.Q. Wu, K. Oikawa, H. Hidaka, N. Serpone, Photoassisted degradation of dye pollutants. 3. Degradation of the cationic dye rhodamine B in aqueous anionic surfactant/TiO_2 dispersions under visible light irradiation: evidence for the need of substrate adsorption on TiO_2 particles, Environ. Sci. Technol. 32 (1998) 2394–2400.
[8] Y.M. Xu, C.H. Langford, UV- or visible-light-induced degradation of X3B on TiO_2 nanoparticles: the influence of adsorption, Langmuir 17 (2001) 897–902.
[9] H. Tada, M. Yamamoto, S. Ito, Promoting effect of MgO_x submonolayer coverage of TiO_2 on the photoinduced oxidation of anionic surfactants, Langmuir 15 (1999) 3699–3702.
[10] M.A. Fox, M.T. Dulay, Heterogeneous photocatalysis, Chem. Rev. 93 (1993) 341–357.
[11] T.S. Yang, M.C. Yang, C.B. Shiu, W.K. Chang, M.S. Wong, Effect of N_2 ion flux on the photocatalysis of nitrogen-doped titanium oxide films by electron-beam evaporation, Appl. Surf. Sci. 252 (2006) 3729–3736.
[12] J.J. Xu, Y.H. Ao, D.G. Fu, C.W. Yuan, Low-temperature preparation of F-doped TiO_2 film and its photocatalytic activity under solar light, Appl. Surf. Sci. 254 (2008) 3033–3038.
[13] A.R. Gandhe, J.B. Fernandes, A simple method to synthezise N-doped rutile titania with enhanced photocatalytic activity in sunlight, J. Solid State Chem. 178 (2005) 2953–2957.
[14] J.C. Yu, W.K. Ho, J.G. Yu, H. Yip, P.K. Wong, J.C. Zhao, Efficient visible-light-induced photocatalytic disinfection on sulfur-doped nanocrystalline titania, Environ. Sci. Technol. 39 (2005) 1175–1179.
[15] B. Neumann, P. Bogdanoff, H. Tributsch, S. Sakthivel, H. Kisch, Electrochemical mass spectroscopic and surface photovoltage studies of catalytic water photooxidation by undoped and carbon-doped titania, J. Phys. Chem. B 109 (2005) 16579–16586.
[16] Y. Du, M. Du, Y. Qiao, J. Dai, J. Xu, P. Yang, Ce(4+) doped TiO_2 thin films: characterization and photocatalysis, Colloid J. 69 (2007) 695–699.
[17] A.M.T. Silva, C.G. Silva, G. Drazic, J.L. Faria, Ce-doped TiO_2 for photocatalytic degradation of chlorophenol, Catal. Today 144 (2009) 13–18.
[18] T.Z. Tong, J.L. Zhang, B.Z. Tian, F. Chen, D.N. He, M. Anpo, Preparation of Ce-TiO_2 catalysts by controlled hydrolysis of titanium alkoxide based on esterification reaction and study on its photocatalytic activity, J. Colloid Interface Sci. 315 (2007) 382–388.
[19] X.Z. Shen, Z.C. Liu, S.M. Xie, J. Guo, Degradation of nitrobenzene using titania photocatalyst co-doped with nitrogen and cerium under visible light illumination, J. Hazard. Mater. 162 (2009) 1193–1198.
[20] Q.F. Chen, D. Jiang, W.M. Shi, D. Wu, Y. Xu, Visible-light-activated Ce–Si co-doped TiO_2 photocatalyst, Appl. Surf. Sci. 255 (2009) 7918–7924.
[21] S. Guo, Z.B. Wu, H.Q. Wang, F. Dong, Synthesis of mesoporous TiO_2 nanorods via a mild template-free sonochemical route and their photocatalytic performances, Catal. Commun. 10 (2009) 1766–1770.
[22] Z.B. Wu, F. Dong, W.R. Zhao, H.Q. Wang, Y. Liu, B.H. Guan, The fabrication and characterization of novel carbon doped TiO_2 nanotubes, nanowires and nanorods with high visible light photocatalytic activity, Nanotechnology 20 (2009) 235701.
[23] K.Y. Cheung, C.T. Yip, A.B. Djurisic, Y.H. Leung, W.K. Chan, Long K-doped titania and titanate nanowires on Ti foil and fluorine-doped tin oxide/quartz substrates for solar-cell applications, Adv. Funct. Mater. 17 (2007) 555–562.
[24] B.X. Wang, Y. Shi, D.F. Xie, Large aspect ratio titanate nanowire prepared by monodispersed titania submicron sphere via simple wet-chemical reactions, J. Solid State Chem. 180 (2007) 1028–1037.
[25] Y.B. Xie, L.M. Zhou, H.T. Huang, Bioelectrocatalytic application of titania nanotube array for molecule detection, Biosens. Bioelectron. 22 (2007) 2812–2818.
[26] Z.Y. Liu, V. Subramania, M. Misra, Vertically oriented TiO_2 nanotube arrays grown on Ti meshes for flexible dye-sensitized solar cells, J. Phys. Chem. B 113 (2009) 14028–14033.
[27] J.G. Yu, S.W. Liu, H.G. Yu, Microstructures and photoactivity of mesoporous anatase hollow microspheres fabricated by fluoride-mediated self-transformation, J. Catal. 249 (2007) 59–66.
[28] Y.B. Xie, C.W. Yuan, Visible-light responsive cerium ion modified titania sol and nanocrystallites for X-3B dye photodegradation, Appl. Catal. B 46 (2003) 251–257.
[29] Y.H. Xu, H.R. Chen, Z.X. Zeng, B. Lei, Investigation on mechanism of photocatalytic activity enahancement of nanometer cerium-doped titania, Appl. Surf. Sci. 252 (2006) 8565–8570.
[30] A.W. Xu, Y. Gao, H.Q. Liu, The preparation, characterization, and their photocatalytic activities of rare-earth-doped TiO_2 nanoparticles, J. Catal. 207 (2002) 151–157.
[31] C.K. Xu, R. Killmeyer, L.M. Gray, S.U.M. Khan, Photocatalytic effect of carbon-modified n-TiO_2 nanoparticles under visible light illumination, Appl. Catal. B 64 (2006) 312–317.
[32] D. Li, H. Haneda, N.K. Labhsetwar, S. Hishita, N. Ohashi, Visible-light-driven photocatalysis on fluorine-doped TiO_2 powders by the creation of surface oxygen vacancies, Chem. Phys. Lett. 401 (2005) 579–584.
[33] G.Q. Li, C.Y. Liu, Y. Liu, Different effects of cerium ions doping on properties of anatase and rutile TiO_2, Appl. Surf. Sci. 253 (2006) 2481–2486.
[34] Q.Z. Yan, X.T. Su, Z.Y. Huang, C.C. Ge, Sol–gel auto-igniting synthesis and structural property of cerium-doped titanium dioxide nanosized powders, J. Eur. Ceram. Soc. 26 (2006) 915–921.
[35] J. Matos, J. Laine, J.M. Herrmann, Effect of the type of activated carbons on the photocatalytic degradation of aqueous organic pollutants by UV-irradiated titania, J. Catal. 200 (2001) 10–20.